Absolute Velocity in the Labrador Sea:

ADCP Observations Along AR7W

Melinda M. Hall and Daniel J. Torres, Woods Hole Oceanographic Institution, Woods Hole, MA 02543

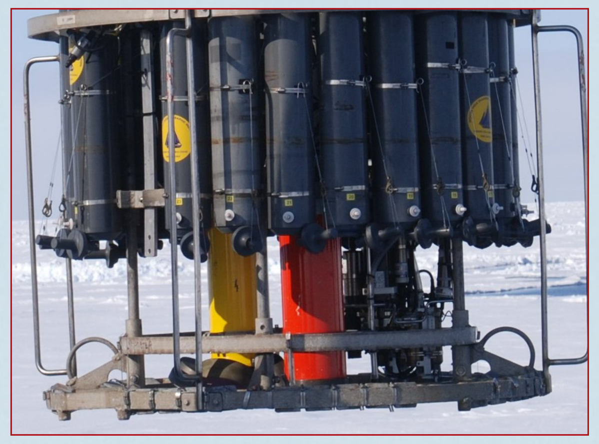

Typical BB150 configuration with external battery pack. (Photo by Daniel Torres)

The subpolar seas of the North Atlantic have long been recognized as important sites of water mass formation and modification. To measure the interannual variability of convection and hydrographic properties in the Labrador Sea, the WOCE/CLIVAR repeat hydrographic line AR7W has been occupied almost yearly since 1990 by investigators at Bedford Institute of Oceanography in Dartmouth, Nova Scotia. This line crosses the Labrador Sea from the east coast of Labrador northeastward to the west coast of Greenland. Since 1995, lowered and shipboard ADCP data have been collected in addition to the hydrographic data. The velocity data remained largely unprocessed and unexamined until now: Here we present directly measured velocities from AR7W for cruises made during springtime of 1995, 1996 and 1998.

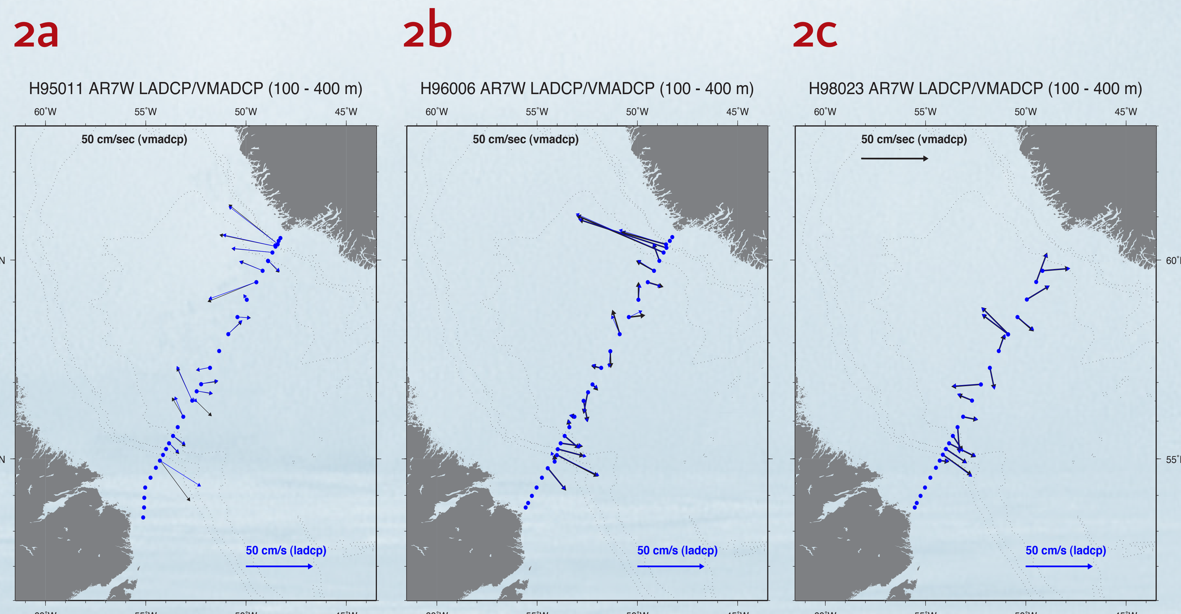

A single downward-facing 150 kHz broadband ADCP was used to collect all the lowered ADCP (LADCP) data for each cruise. The LADCP was typically set up to collect 16 meter depth cells of single ping ensembles. The data have been processed following the method described by Firing and Gordon (1990) and Fischer and Visbeck (1993). The basic process involves first differentiating each velocity profile relative to depth to obtain a full depth shear profile. Depth of the package is obtained from the CTD pressure sensor (or integrating vertical velocity if sensor is unavailable). The shear profile is carefully edited for outliers, averaged into depth bins (usually 10 - 20 meters), and integrated to obtain the baroclinic component of absolute velocity. GPS data from the start and end of the cast are used to obtain the barotropic component of the velocity profile. The two are combined to obtain a final absolute velocity profile for the full water column. Recent enhancements in the Visbeck software utilize an inverse solution which incorporates the additional use of bottom tracking and SADCP data to constrain the shear profile (Visbeck, 2002). Figures 2a-c compare the LADCP and SADCP vector velocities averaged over the depth range 100-400 meters. Generally speaking, these should be nearly identical because of the processing method. Differences may arise in some cases when SADCP cannot be used to constrain the LADCP data.

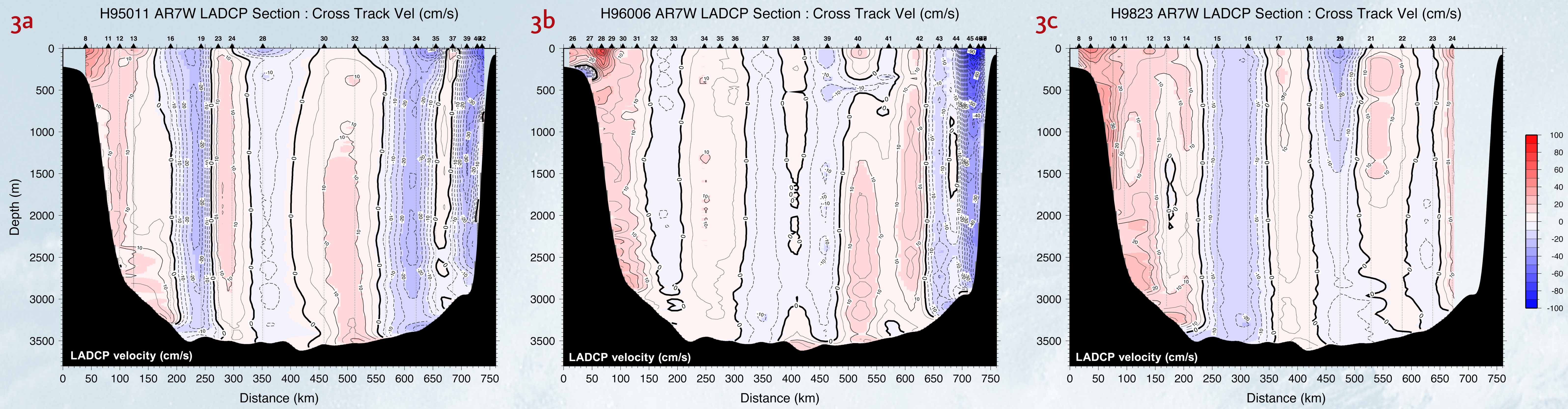

The general circulation of the Labrador Sea consists of a boundary current system circling the rim of the basin cyclonically (comprising various shallow and deep components) and an interior circulation characterized by barotropic, elongated recirculation cells as well as a spatially variable, active eddy field. The boundary currents can be seen in both the shallow vector velocity plots (Figure 2) as well as the sections of cross-track velocity presented for each of these years (Figure 3 a, b, c). Velocities have been rotated 60 degrees counterclockwise from due east, as this is roughly the angle of the AR7W line; positive cross-track velocities are towards the northwest. We also show depth-integrated, cumulative transport going from Labrador to Greenland (Figure 4). In 1998, the boundary current transport along Labrador appears to be nearly twice as strong as in the other two years, almost 60 Sv vs. roughly 30 Sv. The 1998 section missed the eastern boundary current; the 1995 and 1996 sections show a very strong, 60-70 Sv current flowing northwestward there. Interior velocities differ for all three years.

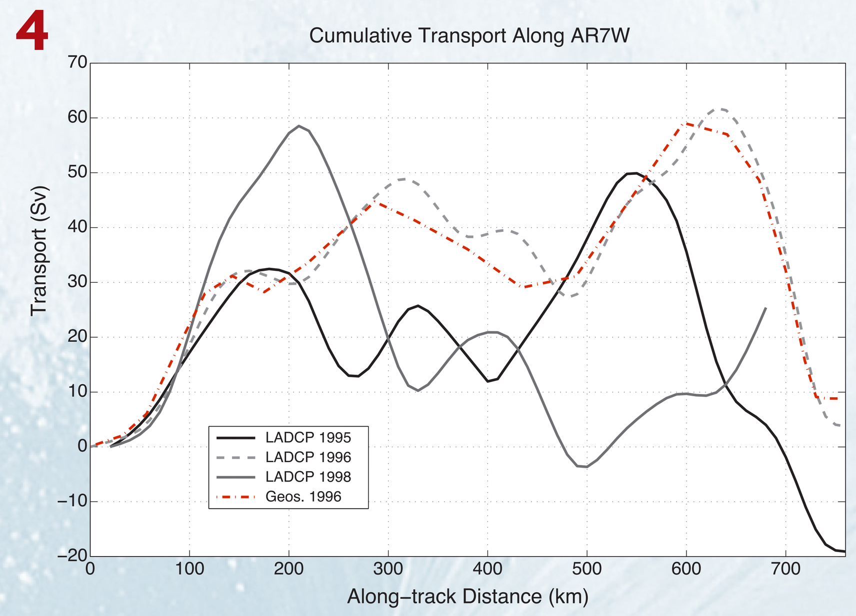

The barotropic nature of the flow, especially in the basin interior, means that geostrophic velocities calculated from hydrographic data alone are inadequate for defining the total velocity field, as there is no appropriate "reference level of no motion." Here we compare the geostrophic and directly measured velocity fields, using the latter to compute barotropic reference velocities for the former. In 1996, the directly observed LADCP velocities yield a nearly-balanced top-to-bottom circulation (Figure 4), meaning that few additional adjustments to geostrophic velocities should be necessary beyond matching them to the LADCP.

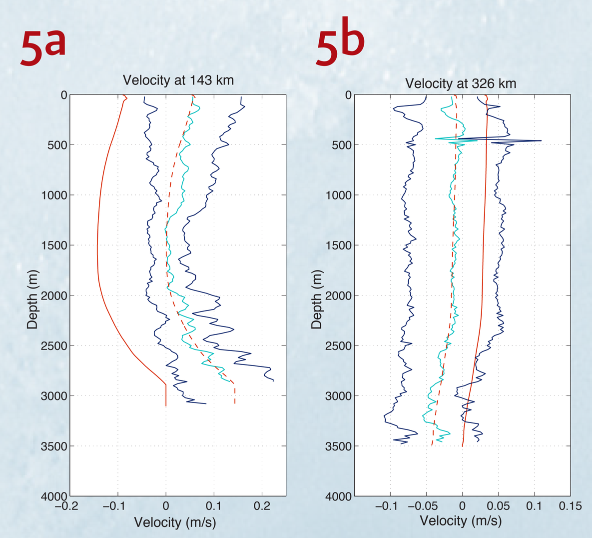

Figure 5 shows 2 examples of computing the barotropic adjustment to the geostrophic velocities. The solid red curve is geostrophic velocity referenced to the bottom; the dark blue ones are the 2 LADCP profiles at the CTD stations used in the geostrophic calculation, while the light blue is the mean of these profiles; the dashed red curve is geostrophic velocity adjusted to match the average LADCP velocity. Figure 5a (left) demonstrates a case in the western boundary current, where significant shear is seen in both velocity measurements, and velocity is weakest at mid-depths. Figure 5b (right) occurs in a region of weak interior flow: shear is weak in all velocity measurements, and LADCP velocities at the 2 stations are opposite signs, yielding weak velocity overall. Referencing each geostrophic velocity profile in a similar way, we construct an absolute geostrophic velocity section for 1996 (Figure 6): the boundary currents are plainly visible, but by comparison with the LADCP velocities, there is much less vertical structure in the interior of the flow for the geostrophic section.

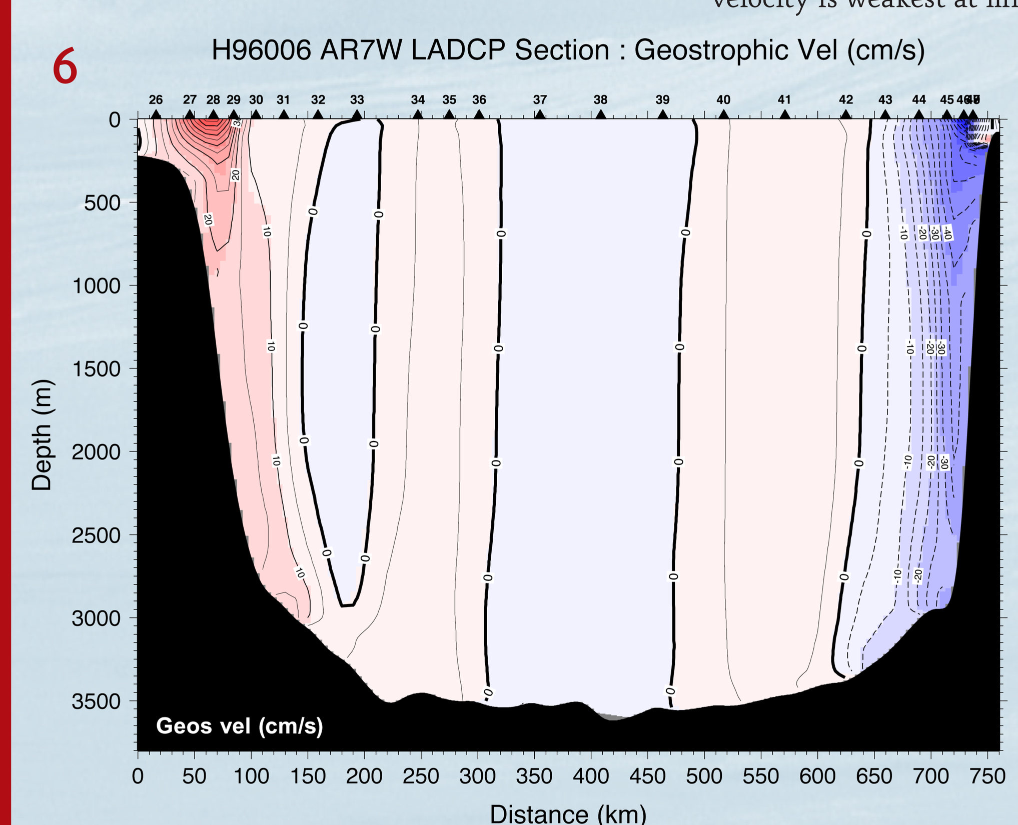

Nevertheless, because the transport is dominated by the strong barotropic contributions, the cumulative transport for geostrophic velocity is quite similar to that for the LADCP (compare red and gray dashed curves in Figure 4). In the future, the construction of absolute velocity sections will be further refined by taking into consideration conservation of mass and water properties, since inflow and outflow poleward of AR7W is limited.

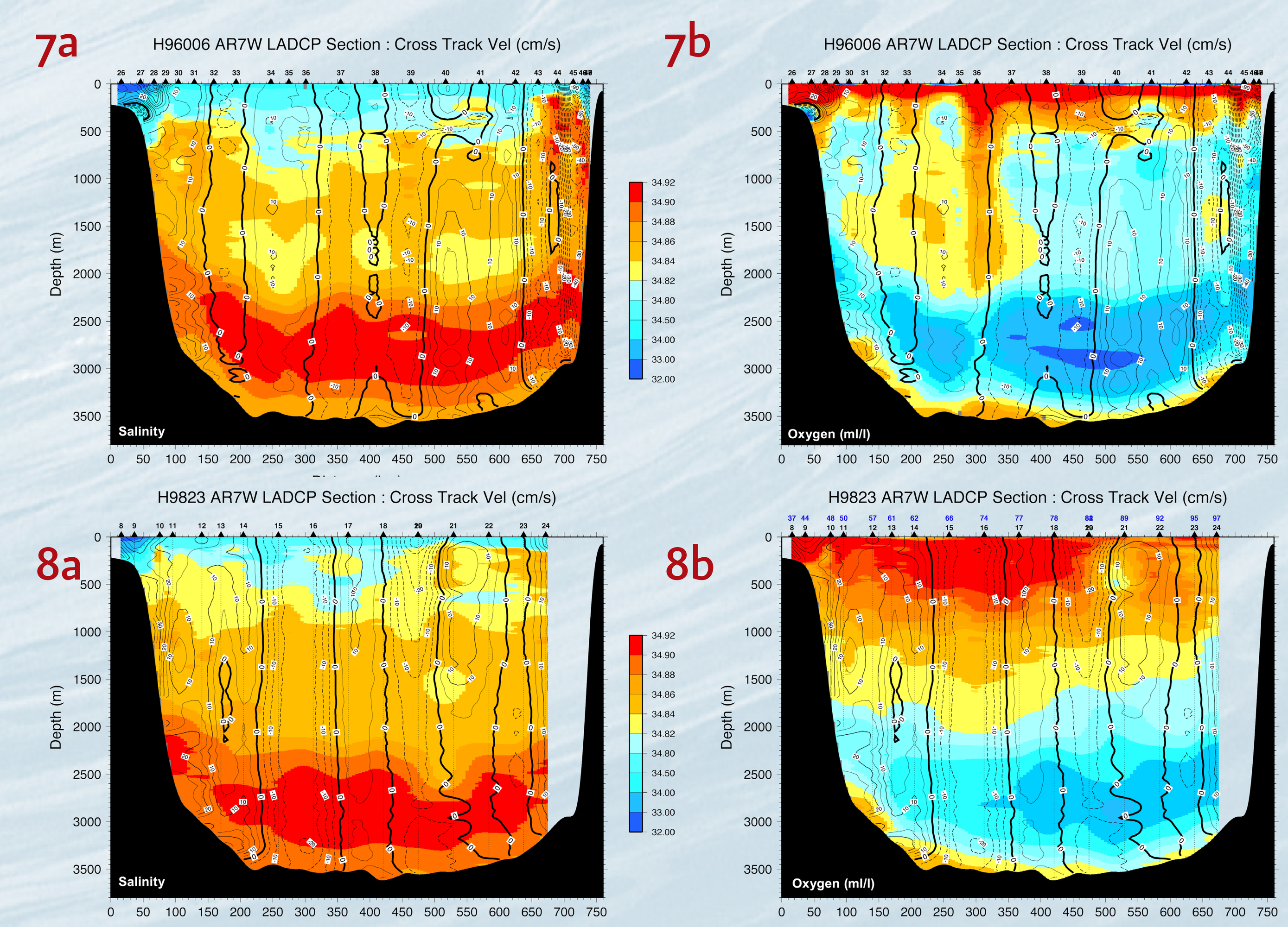

Finally, we briefly show the salinity and oxygen for 1996 and 1998, with the cross-track velocities superimposed (Fig. 7a, b; Fig. 8a, b). The salinity minima near 1500 m depth in 1996 have largely disappeared by 1998, and the bottom salinity has increased slightly as well. Oxygen shows different patterns of change. We have not yet had the opportunity to fully investigate the relationship between changes in the property and velocity fields. We plan to continue these investigations with the many additional AR7W crossings for which there are ADCP data.

Acknowledgments

We would like to thank the many individuals whose cooperation has made the collection of this dataset possible. We especially thank Allyn Clarke, John Lazier, John Loder, Ross Hendry, Igor Yashayaev, and Murray Scotney. This work was supported by NSF Grant OCE-0622640.

References

Firing, E., and L. Gordon, 1990. Deep ocean acoustic doppler current profiling. *Proc. IEEE Fourth Working Conf. on Current Measurements*, Clinton, MD, Current Measurement Technology Committee of the Ocean Engineering Society, 192–201.

Fischer, J., and M. Visbeck, 1993. Deep velocity profiling with self-contained ADCPs. *J. Atmos. Oceanic Technol.*, **10**, 764–773.

Visbeck. M., 2002. Deep velocity profiling using lowered acoustic Doppler current profilers: Bottom track and inverse solutions. *Journal of Atmospheric and Oceanic Technology*, **19**, 794-807.